Supplementary Materials

Facile Construction of Porous ZnMn$_2$O$_4$ Hollow Micro-Rods as Advanced Anode Material for Lithium Ion Batteries

Yuyan Wang †, Senyang Xu †, Yamin Zhang, Linrui Hou * and Changzhou Yuan *

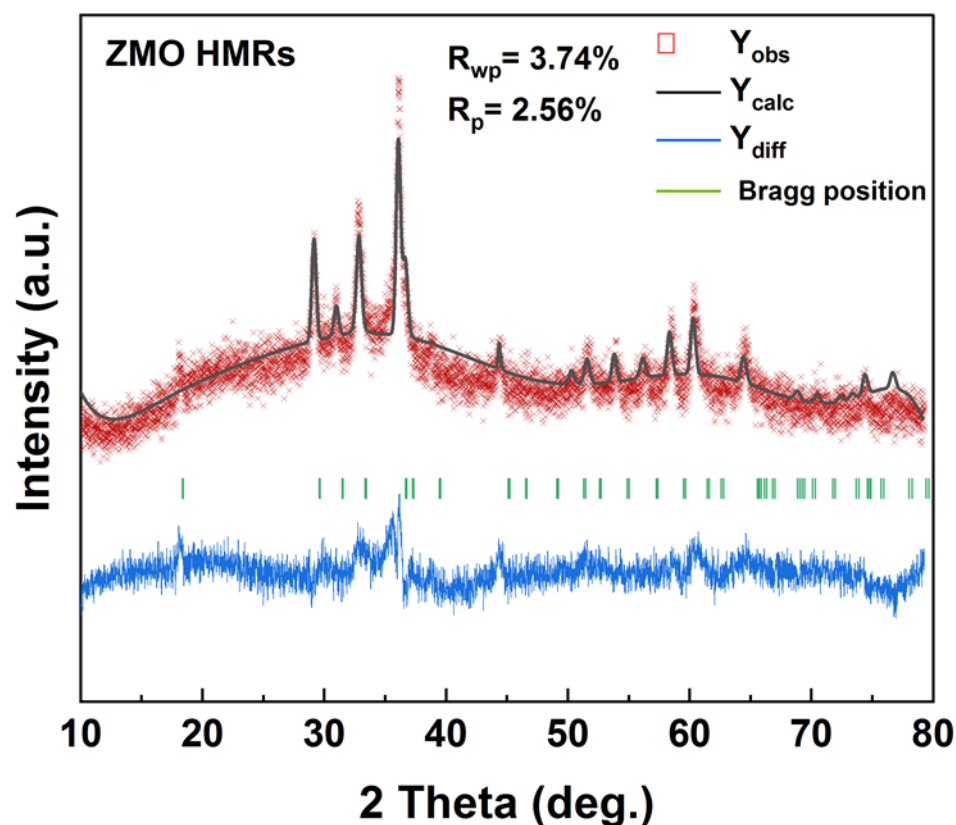School of Materials Science & Engineering, University of Jinan, Jinan 250022, China
* Correspondence: mse_houlr@ujn.edu.cn (L.H.); mse_yuancz@ujn.edu.cn (C.Y.)
† Theses authors contributed equally to this work.

Figure S1. Rietveld-refined XRD pattern of ZnMn$_2$O$_4$.

Table S1. Rietveld refinement results of XRD data for ZMO HMRs samples.

	a (Å)	b (Å)	c (Å)	volume (Å^3)	R$_{wp}$ (%)	R$_P$ (%)	CHI^2
ZMO HMRs	5.6533	5.6533	8.9989	287.612	3.74	2.56	2.882

Figure S2. (**a**, **b**) FESEM and (**c**, **d**) TEM images for the ZnC_2O_4-$MnC_2O_4 \cdot 2H_2O$ precursor.

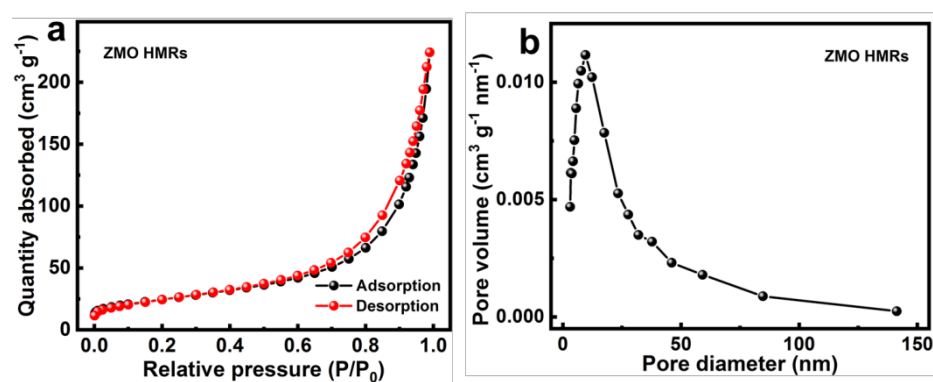**Figure S3.** TG-DSC curves of the ZnC_2O_4-$MnC_2O_4 \cdot 2H_2O$ precursor.

Figure S4. (**a**) Nitrogen adsorption/desorption isotherms and (**b**) pore-size distribution plot of the ZMO HMRs.
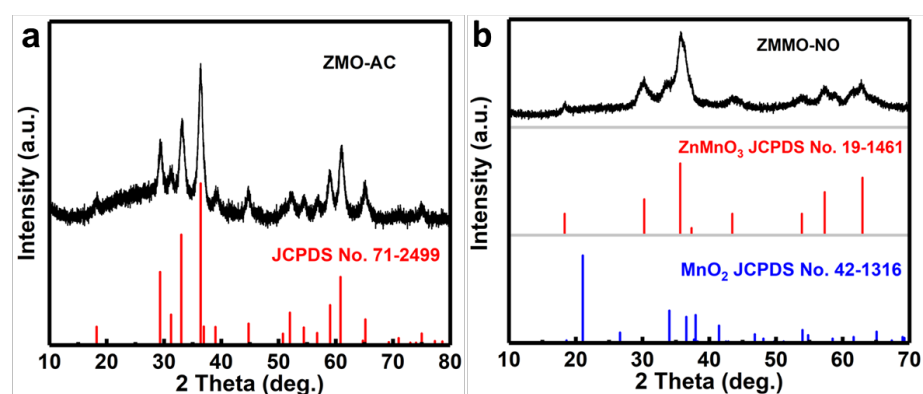
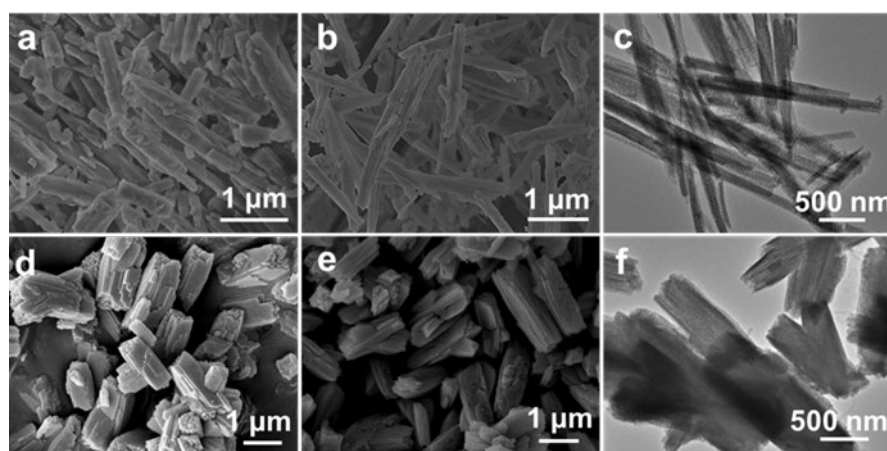**Figure S5.** The XRD pattern of ZMO-AC (**a**) and (**b**) ZMMO-NO.

Figure S6. FESEM images of the ZMO-AC: (**a**) precursor, (**b**) after annealing, (**c**) TEM images for after annealing. ZMO-NO: (**d**) precursor, (**e**) after annealing, (**f**) TEM images for after annealing.
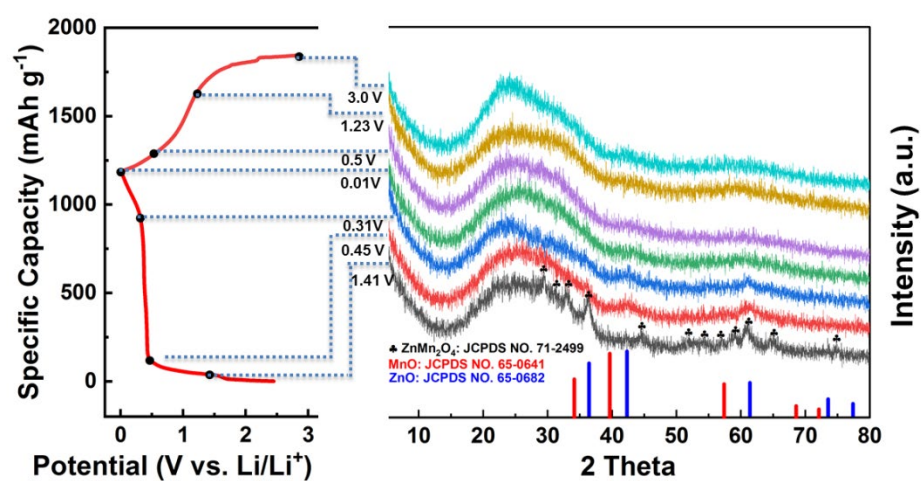

Figure S7. Typical initial discharge-charge voltage profiles of the ZMO HMRs electrode and corresponding ex-situ XRD analysis at different selected voltages.
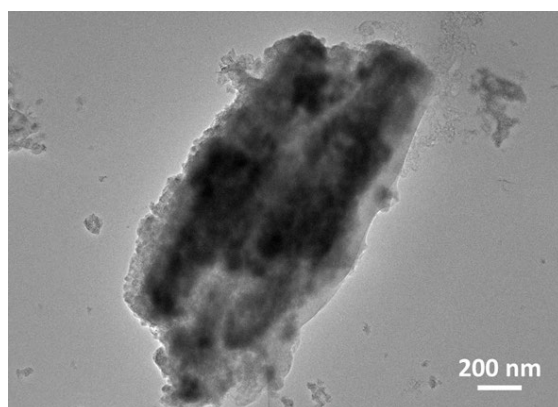
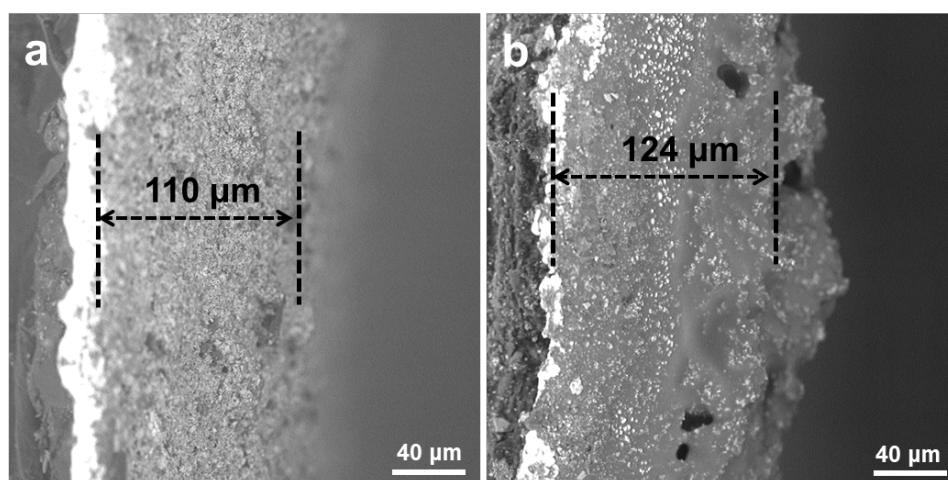**Figure S8.** FESEM image of the ZMO-HMRs cycled over 250 cycles.

Figure S9. Cross-section SEM images of (**a**) original pristine ZMO HMRs electrode, (**b**) pristine ZMO HMRs electrode after 250 cycles at 0.5 A g$^{-1.}$
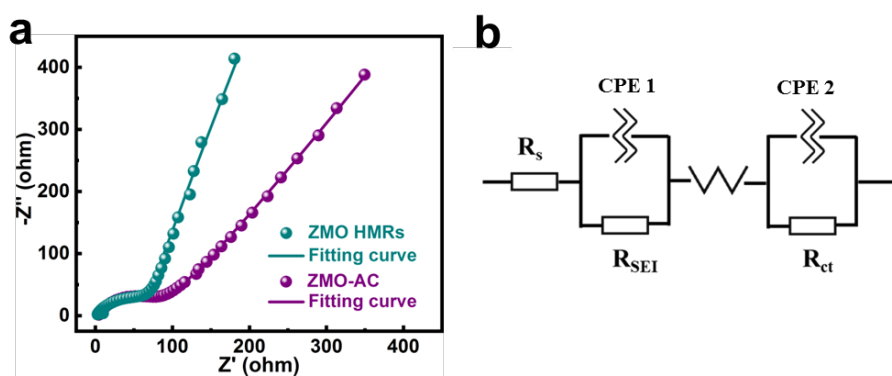

Figure S10. (**a**) EIS spectra and (**b**) corresponding equivalent circuit of ZMO HMRs and ZMO-AC.

Table S2. Corresponding EIS fitted data for the ZMO HMRs and ZMO-AC.

Electrode	R$_S$ (Ω)	CPE 1 (Ω)	R$_{SEI}$ (Ω)	W (Ω)	CPE 2 (Ω)
ZMO HMRs	1.616	0.6922	97.56	160.0	0.7896
ZMO-AC	3.183	0.6925	106.4	206.2	0.6719